

RESEARCH

Open Access



Deciphering the dynamics and trophic mode distribution of the leaf spot-associated fungal community of eggplant (*Solanum melongena* L.)

Arya Kaniyassery¹, Sudhanva Bhimanakatte Sathish¹, Sachin Ashok Thorat¹, Thokur Sreepathy Murali²,
Mattu Radhakrishna Rao³ and Annamalai Muthusamy^{1*} 

Abstract

The invasion of phytopathogens impacts the composition and associations of the internal microbial inhabitants. Leaf spot is one of the most devastating diseases in eggplant var. Mattu Gulla which is unique in terms of geographic indication (GI) status. Leaf spot samples (asymptomatic and symptomatic) were collected to characterize the fungal community associated with them using culture-based and next-generation ITS rRNA-based metabarcoding approaches. Both methods showed that Ascomycota and Basidiomycota were the predominant phyla in both groups. In the asymptomatic group, Didymosphaeriaceae, Pleosporaceae, Trichomeriaceae, and Capnodiaceae were the most differentially abundant families. In contrast, Phaeosphaeriaceae, Pleosporaceae, Didymellaceae, Rhynchogastremataceae, and Bulleribasidiaceae were the most differentially abundant families in the symptomatic group. At the genus level, *Cladosporium* was the most differentially abundant genus in the asymptomatic group. In the symptomatic group *Alternaria*, *Remotididymella*, *Vishniacozyma*, *Bulleribasidium*, *Occultifur*, *Epicoccum*, and *Loratospora* were the abundant genera. The pathotroph-saprotrophic mode was the most common mode identified in both groups, with an increased abundance in the symptomatic group. Seven fungal families and two genera were identified as common according to the culture-based method and NGS analysis based on ITS rRNA metabarcoding. Our study indicated that the composition of the core microbial community varies with plant health status, and a combination of culturable and next-generation ITS rRNA-based metabarcoding approaches could be a reliable option for obtaining a detailed understanding of plant-associated fungal communities.

Keywords Eggplant, Leaf spot, ITS, Metabarcoding, Fungal community, Trophic mode

Background

Microbial communities are abundant and diverse in plants and are referred to as the second genome of the plant (Zhang et al. 2021). They are an essential component of the host and are widely acknowledged to serve crucial functions in plant development and health (Gao et al. 2021). Many biotic and abiotic factors, including host attributes [for example, plant compartment and host genetics] (Edwards et al. 2015; Agler et al. 2016; Xiong et al. 2021), climate, and soil type (Laforest-Lapointe et al. 2016; De Vries et al. 2018), influence the establishment of the plant microbiome. Meta-analyses

*Correspondence:

Annamalai Muthusamy
a.msamy@manipal.edu

¹ Department of Plant Sciences, Manipal School of Life Sciences, Manipal Academy of Higher Education (MAHE), Manipal, Karnataka 576104, India

² Department of Public Health Genomics, Manipal School of Life Sciences, Manipal Academy of Higher Education (MAHE), Manipal, Karnataka 576104, India

³ Pragathi, Bhavani Nagar, Alevoor Road, Manipal, Karnataka 576104, India



© The Author(s) 2024. **Open Access** This article is licensed under a Creative Commons Attribution 4.0 International License, which permits use, sharing, adaptation, distribution and reproduction in any medium or format, as long as you give appropriate credit to the original author(s) and the source, provide a link to the Creative Commons licence, and indicate if changes were made. The images or other third party material in this article are included in the article's Creative Commons licence, unless indicated otherwise in a credit line to the material. If material is not included in the article's Creative Commons licence and your intended use is not permitted by statutory regulation or exceeds the permitted use, you will need to obtain permission directly from the copyright holder. To view a copy of this licence, visit <http://creativecommons.org/licenses/by/4.0/>.

of microbial datasets associated with plant disease and health would help us comprehend the influence of microbiomes on their host and the intricate interactions that shape the host's fitness and survival (Ginnan et al. 2018). Invasion of phytopathogens causes changes in the composition and associations of the internal microbial inhabitants and impacts the behavior of other plant pathogens (Wang et al. 2017; Li et al. 2019). In recent years, there has been a growing reliance on culture-independent techniques for characterizing microbial communities, primarily due to their practical advantages. The key benefit of these methods lies in their ability to easily identify a significant portion of microbial diversity that may be challenging to observe through traditional culture-based studies. While current culture-based methods have limitations in detecting various types of organisms, they excel in quantifying the absolute cell abundances of living microbes that can be cultured (Zapka et al. 2017; Krstić Tomić et al. 2023).

Eggplant (*Solanum melongena* L.) is an economically important crop cultivated in India, with Asia accounting for 94% of global production (Aumentado and Balendres 2022). Mattu Gulla is a variety with geographical indication status in 2011 cultivated at Mattu village in Udupi district, Karnataka, India, for 500 years (Bhat and Madhyastha 2007). It is known for its legacy, unique physical appearance, and bioactive metabolites in fruits (Swathy et al. 2023). Plant diseases caused by fungal pathogens result in significant yield reductions and pose serious challenges to global food production (Seybold et al. 2020). Leaf spot disease was prevalent in the Mattu Gulla fields in survey during 2018–2019 and 2019–2020 (Kaniyassery et al. 2024). *Alternaria*, *Cercospora*, and *Septoria* are reported to be the predominant fungal genera that cause leaf spot disease in eggplant (Kaniyassery et al. 2023).

The phyllosphere (aboveground plant parts, usually the leaf surface) is a crucial plant environment inhabited by distinct microbial species (Bringel and Couée 2015). Phyllosphere microorganisms can impact host fitness by producing plant hormones/plant growth regulators and inducing defense responses against pathogen invasion (Ritpitakphong et al. 2016; Venkatachalam et al. 2016). Although the mode of action of individual pathogens has been extensively studied, little is known about the role of the larger fungal communities associated with plants in the modulation of diseases or how their diversity and abundance are altered when a pathogen invades a plant (Blackwell 2011; Hacquard and Schadt 2015). Microbes defend plants from infections through various methods, including niche competition, antibiotic production, the release of secondary metabolites, and the development of systemic resistance, which boost plant defenses in

preparation for pathogen invasion (Carvalho and Castillo 2018). Pathobiome research now offers the chance to investigate the dynamics of the plant micro(patho)biome, the kinds of interactions with the plant, interactions and/or competition between related bacteria, the slow assembly of harmful microbes, and the ensuing pathogenesis or disease manifestation (Dastogeer et al. 2022; Mehrotra et al. 2024). This is particularly significant in the case of protected indigenous varieties such as Mattu Gulla, where the scope of improving agronomically favorable traits through modern breeding methods is limited due to their traditional importance. The study of the functional characteristics of phyllosphere microorganisms has focused primarily on the cultivable portion of the leaf microflora. Recent advances in next-generation sequencing (NGS) platforms and related computational tools for large-scale analysis have made it possible to explore unculturable portions of the microflora (Lundberg et al. 2012).

Considering the importance of beneficial plant-microbiome interactions, this study aimed to (1) identify leaf spot-associated culturable fungi, (2) compare the variation in leaf microbial communities in symptomatic samples with that in asymptomatic samples using NGS analysis, (3) predict trophic modes of microbial community from ITS rRNA profiles, and (4) compare and analyze fungal profiles from traditional culturing and isolation methods and metabarcoding approach.

Results

Isolation and identification of leaf spot-associated fungi

To identify the culturable fungi in the leaves of eggplant var. Mattu Gulla affected by leaf spot disease, leaf samples showing spots with defined margins and brown centers were collected from Mattu Gulla fields, and the associated fungi were isolated. A total of 18 morphologically different fungi were isolated from the samples collected for the culture-based approach. The isolates were identified based on morphology up to the genus level (Additional file 1: Figure S1). ITS sequencing was performed, and identity was confirmed to the species level using a BLAST search against the GenBank database. The sequences showed a percentage similarity from 97 to 100% with the existing sequences in GenBank (Additional file 2: Table S1). The isolates that could not be assigned to the level are referred to as the genus itself.

Fungal composition and distribution in the asymptomatic and symptomatic groups

We performed an NGS analysis of ITS amplicons derived from asymptomatic and symptomatic leaf samples to study the fungal community associated with leaf spots. After sequence processing, a total of 420,623 high-quality

reads from the asymptomatic group and 334,778 from the symptomatic group were ultimately obtained (Additional file 2: Table S2). A total of 334 amplicon sequence variants (ASVs) were obtained, of which 206 were successfully assigned taxonomical identities, and the remaining 128 were unassigned. Among the 206 identified ASVs, genus-level identification was possible for 39 (Additional file 2: Table S5).

Ascomycota (asymptomatic: 57.43% and symptomatic: 76.42%), Basidiomycota (asymptomatic: 29.25% and symptomatic: 9.42%), and Mucoromycota (asymptomatic:

1.33% and symptomatic: 14.14%) were the three major phyla present in the samples (Fig. 1a). The relative abundance of Ascomycota was greater in the symptomatic group than in the asymptomatic group from the same fields (field location 1 asymptomatic [F1C]: 47.16%, field location 2 asymptomatic [F2C]: 37.16%, field location 3 asymptomatic [F3C]: 89.57%; field location 1 symptomatic [F1S]: 57.57%, field location 2 symptomatic [F2S]: 71.69%, field location 3 symptomatic [F3S]: 93.37%) (Additional file 2: Table S3). Basidiomycota was found to be the second major phylum with a high relative

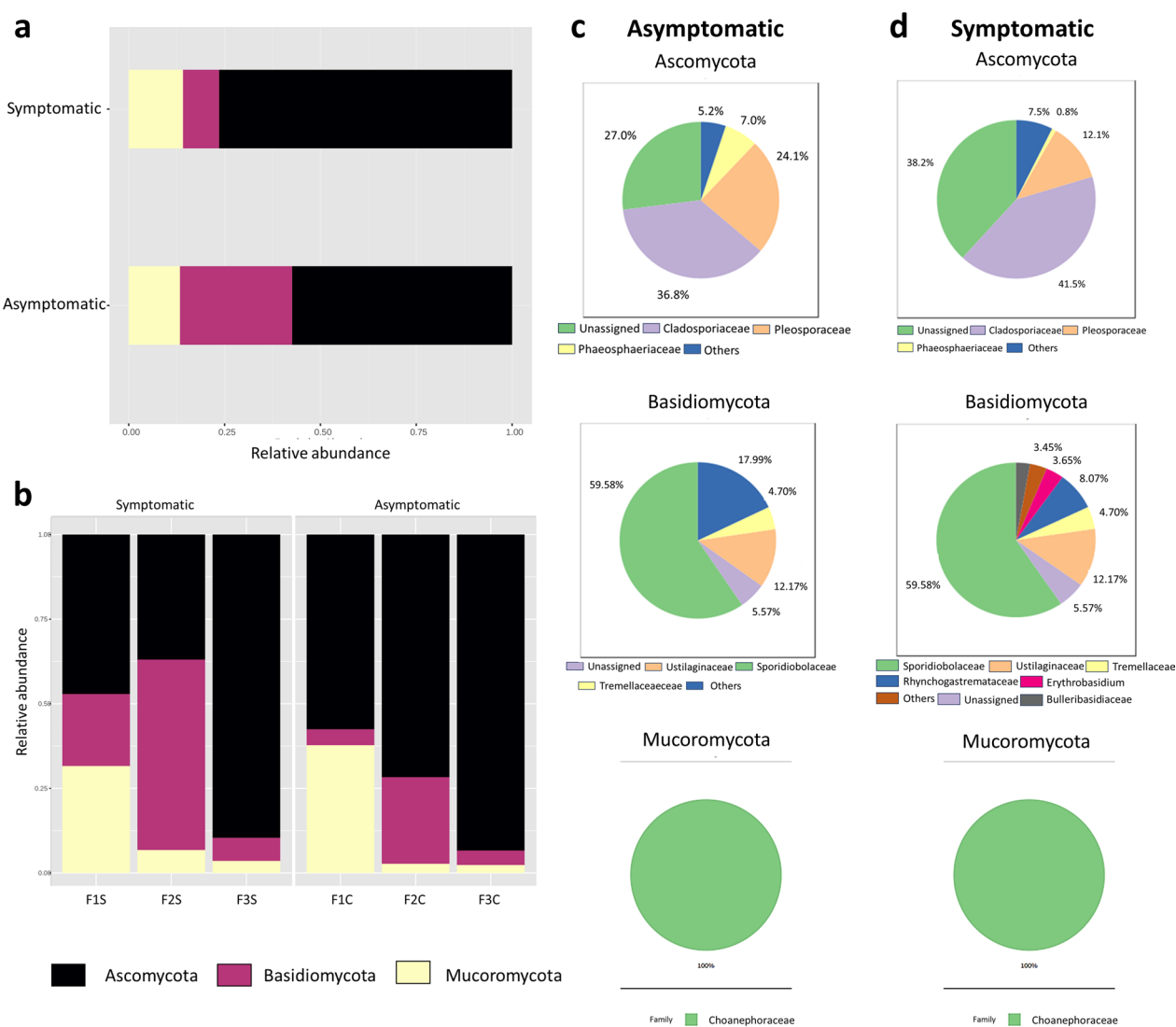


Fig. 1 Proportional distribution of different fungi in the asymptomatic and symptomatic groups. **a, b** The vertical bars represent the relative abundance (%) of different microbial phyla in the two groups. The bars are plotted with respect to the relative taxonomic abundance at phylum level. **c, d** The pie charts show the comparative abundance profiles of both groups at the family level (merged smaller taxa < 0.05) in each phylum across the symptomatic and asymptomatic groups. The phylum Mucoromycota in both groups comprised the Choanephoraceae family (100%). F1C, F2C, and F3C represented asymptomatic group from field locations 1, 2 and 3, respectively; F1S, F2S and F3S represented symptomatic group from field locations 1, 2, and 3, respectively

abundance, and the relative abundance of this phylum was greater in the asymptomatic group than in the symptomatic group from the respective field locations (Fig. 1b, c). Twenty-two different genera were identified from the 39 ASVs. The following genera were highly prevalent in the samples: *Cladosporium* (13 ASV count), *Phaeosphaeria* (11), *Sporobolomyces* (11), *Papiliotrema* (9), *Curvularia* (8), *Alternaria* (6), *Periconia* (6), and *Vishniacozyma* (4) (Additional file 2: Table S1).

The richness and diversity of fungi varied between the asymptomatic and symptomatic groups

Alpha and beta diversity analyses were performed for the 206 ASVs that were taxonomically identified to assess the richness and diversity of fungi. The results of a rarefaction analysis (Additional file 1: Figure S2) demonstrated that the sequencing depth was sufficient to determine the overall species richness across all the samples. The Good's coverage index (99.98% \pm 0.012%) showed that the sequencing results statistically represented the accurate composition of the fungal microbiome (Additional file 2: Table S3). Two samples (F2S and F3S) from the symptomatic group showed increased species richness compared with those from the asymptomatic group (Additional file 1: Figure S2). The Chao1, Shannon, and Simpson alpha diversity indices varied across the asymptomatic and symptomatic groups (Fig. 2, Additional file 2: Table S4). The analysis revealed that the samples from the symptomatic group were relatively more diverse than those from the asymptomatic group. Principal coordinate analysis (PCoA) based on the Bray–Curtis method segregated asymptomatic and symptomatic groups based on the field from which they originated (Fig. 3a). At the family level, the symptomatic group showed noticeable similarity between the samples from the three fields. Nonmetric multidimensional scaling (NMDS) analysis was performed to determine the classification and relationships between the groups, and the samples were segregated (Fig. 3b) (F value: 1.2207; R-squared: 0.23382; p : 0.4). There was no significant difference in beta diversity between the asymptomatic and symptomatic groups.

Abundance of significantly different fungal taxa in symptomatic and asymptomatic samples

ASVs were analyzed for differentially abundant taxa at both the family and genus levels using the DESeq2 software. Nineteen ASVs were significantly enriched, and 18 ASVs were significantly depleted in the asymptomatic group at the family level (Additional file 2: Table S6). At the genus level, 9 ASVs were depleted significantly, and there were no enriched ASVs in the asymptomatic group compared with the symptomatic group. The Pleosporaceae family, belonging to the phylum Ascomycota,

was the most significantly enriched family in the symptomatic group, followed by other families in the phylum Basidiomycota (Fig. 4). *Vishniacozyma*, *Remotididymella*, *Epicoccum*, *Bulleribasidium*, *Alternaria*, *Occultifur*, *Leptospora*, and *Papiliotrema* were the significantly depleted genera in the asymptomatic group.

Subsequently, we performed linear discriminant effect size (LEfSe) analysis using the abundance data to compare the presumed phylotypes of the fungal microbiomes of the asymptomatic and symptomatic groups. The ASVs assigned up to the family level (206 ASVs) and up to the genus level (39 ASVs) were analyzed separately. The cladogram and bar plot highlight several taxa that are significantly enriched in either the symptomatic or asymptomatic samples. Taxa that are differentially abundant in the asymptomatic group are marked in red, while those enriched in the symptomatic group are marked in green (Figs. 5 and 6). Nodes indicate the hierarchical relationships between different taxa, showing which groups are more closely related based on their evolutionary history. Significant nodes often highlight the taxa that are differentially abundant between the symptomatic and asymptomatic groups. LEfSe and LDA revealed that the fungal microbiome of the asymptomatic group was more diverse than that of the symptomatic group. Features that indicated a differential abundance of the fungal microbiome between the asymptomatic and symptomatic groups were computed using a histogram of the LDA scores. The LDA scores indicated that Basidiomycota and Ascomycota were the two most abundant phyla in both groups (Figs. 5 and 6). In the asymptomatic group, Didymosphaeriaceae, Pleosporaceae, Trichomeriaceae, and Capnodiaceae were the most differentially abundant families (Fig. 5). However, in the symptomatic group, Phaeosphaeriaceae, Pleosporaceae, Didymellaceae, Rhynchogastremataceae, and Bulleribasidiaceae were the most differentially abundant families (Fig. 5). At the genus level, *Cladosporium* was the most differentially abundant genus in the asymptomatic group, while in the symptomatic group, *Alternaria*, *Remotididymella*, *Vishniacozyma*, *Bulleribasidium*, *Occultifur*, *Epicoccum* and *Loratospora* were differentially abundant genera (Fig. 6).

Fungal communities were distributed across seven trophic modes

The trophic modes of the fungal community were annotated in both the symptomatic and asymptomatic groups using the FUNGuild tool. A total of 206 ASVs identified at the family level were analyzed using FUNGuild. Seven trophic modes, pathotroph, pathotroph-saprotroph, pathotroph-saprotroph-symbiotroph, pathotroph-symbiotroph, saprotroph, saprotroph-symbiotroph, and symbiotroph, were allocated for the 170 ASVs (Fig. 7), while

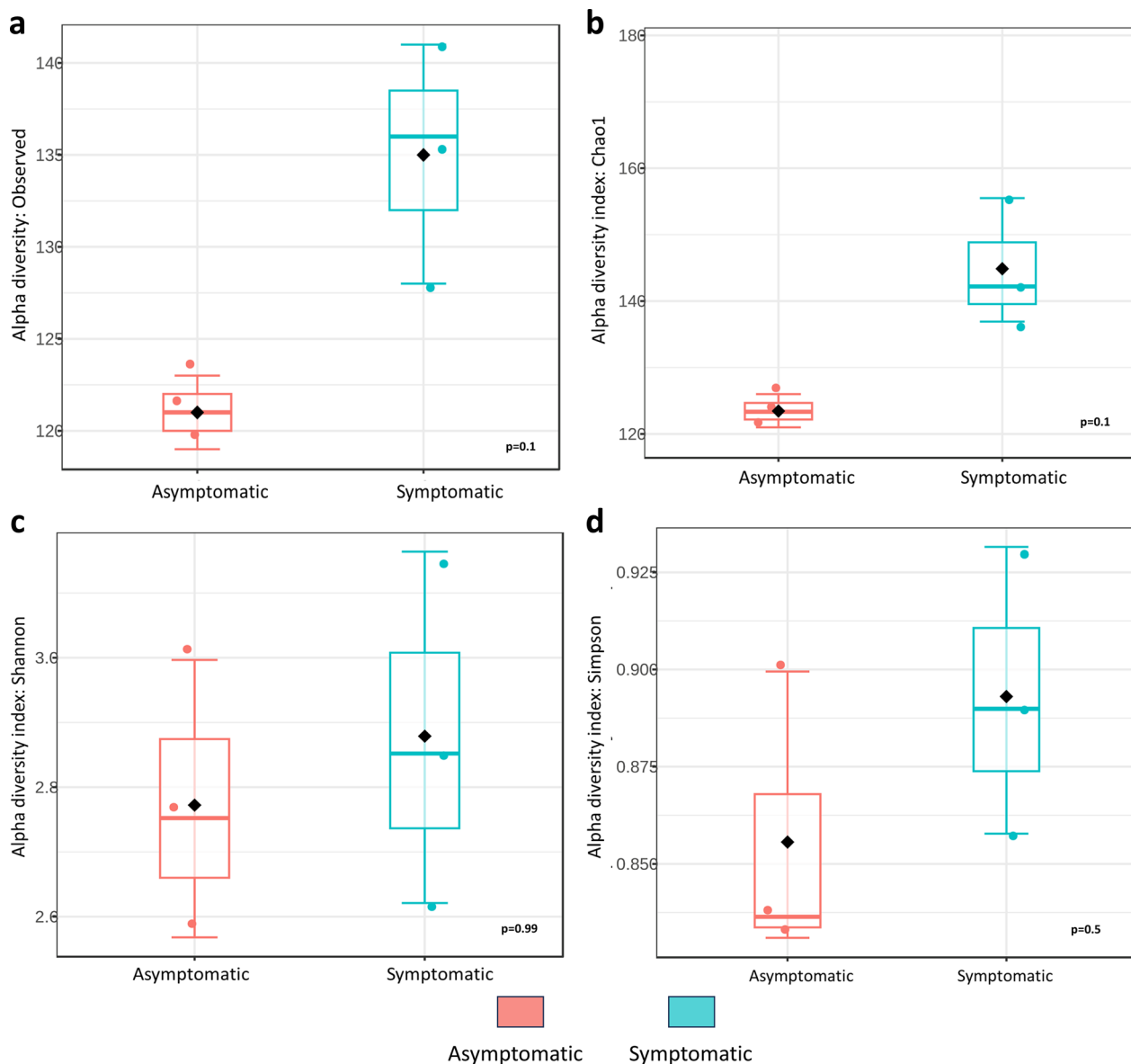


Fig. 2 Fungal diversity in the fungal microbiome of asymptomatic and symptomatic samples. **a** Observed, **b** Chao1 index, **c** Shannon index, **d** Simpson index

the trophic mode could not be assigned for the remaining ASVs. The pathotroph-saprotrophic mode was the most common mode identified in both groups, with an increased abundance in the symptomatic group compared with the asymptomatic group (difference: 18,523 ASV counts). Pathotrophs and pathotrophs-saprotrophs-symbiotrophs were more abundant in asymptomatic samples than in symptomatic leaf samples (differences: 10,794 (pathotrophs) and 11,047 (pathotrophs-saprotrophs-symbiotrophs) ASV counts respectively). Saprotrophs were more abundant in the symptomatic group than in the asymptomatic group (difference: 2141 ASV

count). Pathotroph-symbiotrophs were not observed in the symptomatic group but were represented by two ASVs in the asymptomatic group. Saprotroph-symbiotrophs were characterized by only one ASV but were dominant in asymptomatic samples, with an ASV count of 116, and they were significantly less abundant in the symptomatic group, with a count of 4 (Fig. 7).

PICRUst2 could predict the most regulated metabolic pathways from the ITS profiles. The 30 top MetaCyc pathways per category can be visualized in a heatmap (Additional file 1: Figure S3). Pathways

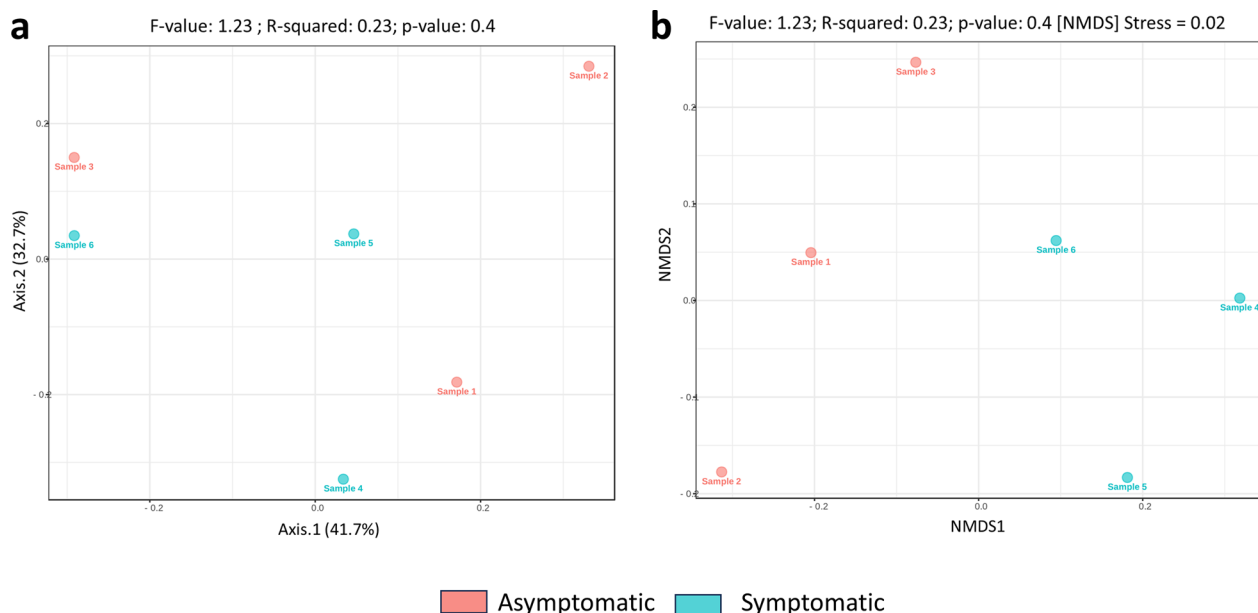


Fig. 3 Beta diversity in the fungal microbiome of asymptomatic and symptomatic samples. **a** PCoA at the feature level. **b** NMDS analysis at the feature level. Samples 1 to 3 represented asymptomatic group from field locations 1, 2, and 3, respectively; Samples 4 to 6 represented symptomatic group from field locations 1, 2, and 3, respectively

whose expression varied between the symptomatic and asymptomatic groups. The pathways that represented the most were the fatty acid elongation pathway and (5Z)-dodec-5-enoate biosynthesis, with increased expression in the symptomatic group compared with the asymptomatic group. The fatty acid elongation pathway is involved in the biosynthesis of long-chain fatty acids, which are essential components of cellular membranes and are crucial for maintaining cell integrity and function. The increased expression of this pathway in symptomatic samples could indicate a cellular response to stress or damage caused by the leaf spot disease. (5Z)-Dodec-5-enoate biosynthesis pathway is related to the biosynthesis of specific fatty acids that can act as signaling molecules or be involved in the synthesis of protective compounds. The increased expression of this pathway in symptomatic samples suggests that it could possibly be produced by compounds that help to combat the pathogen or mitigate damage. The least represented pathway was the L-ornithine biosynthesis pathway, whose expression was greater in the asymptomatic group than in the symptomatic group. L-ornithine is a precursor in the biosynthesis of polyamines, which are involved in various cellular processes, including stress response, cell division, and differentiation. The higher expression of this pathway in the asymptomatic group suggests its role

in maintaining plant health and potentially enhancing resistance to leaf spot disease.

Common families and species for culture method and NGS analysis

The results of the traditional culturing and isolation methods and the metabarcoding approach were compared to understand the similarities and differences in the fungal community structure, as revealed by these two techniques. The family-level taxonomy of the cultured fungal isolates was identified and compared with the ASVs assigned to those families from the NGS analysis. After identifying such ASVs, the abundances were plotted for the asymptomatic and symptomatic groups. The 18 cultured isolates belonged to the phyla Ascomycota and Basidiomycota and were distributed across 11 different families: Nectriaceae, Botryosphaeriaceae, Pleosporaceae, Corynesporascaceae, Aspergillaceae, Hypocreaceae, Xylariaceae, Ceratobasidiaceae, Pleosporaceae, Trichosphaeriaceae, Diaporthaceae, and Glomerellaceae. From these families, 7 families were also detected in the fungal microbiome analysis. The microbiome analysis did not detect Ceratobasidiaceae, Diaporthaceae, Glomerellaceae, or Hypocreaceae. Corynesporascaceae, Aspergillaceae, Xylariaceae, and Trichosphaeriaceae were abundant in the asymptomatic group. In contrast, Nectriaceae, Botryosphaeriaceae, and Pleosporaceae were abundant in the symptomatic

Asymptomatic Vs Symptomatic

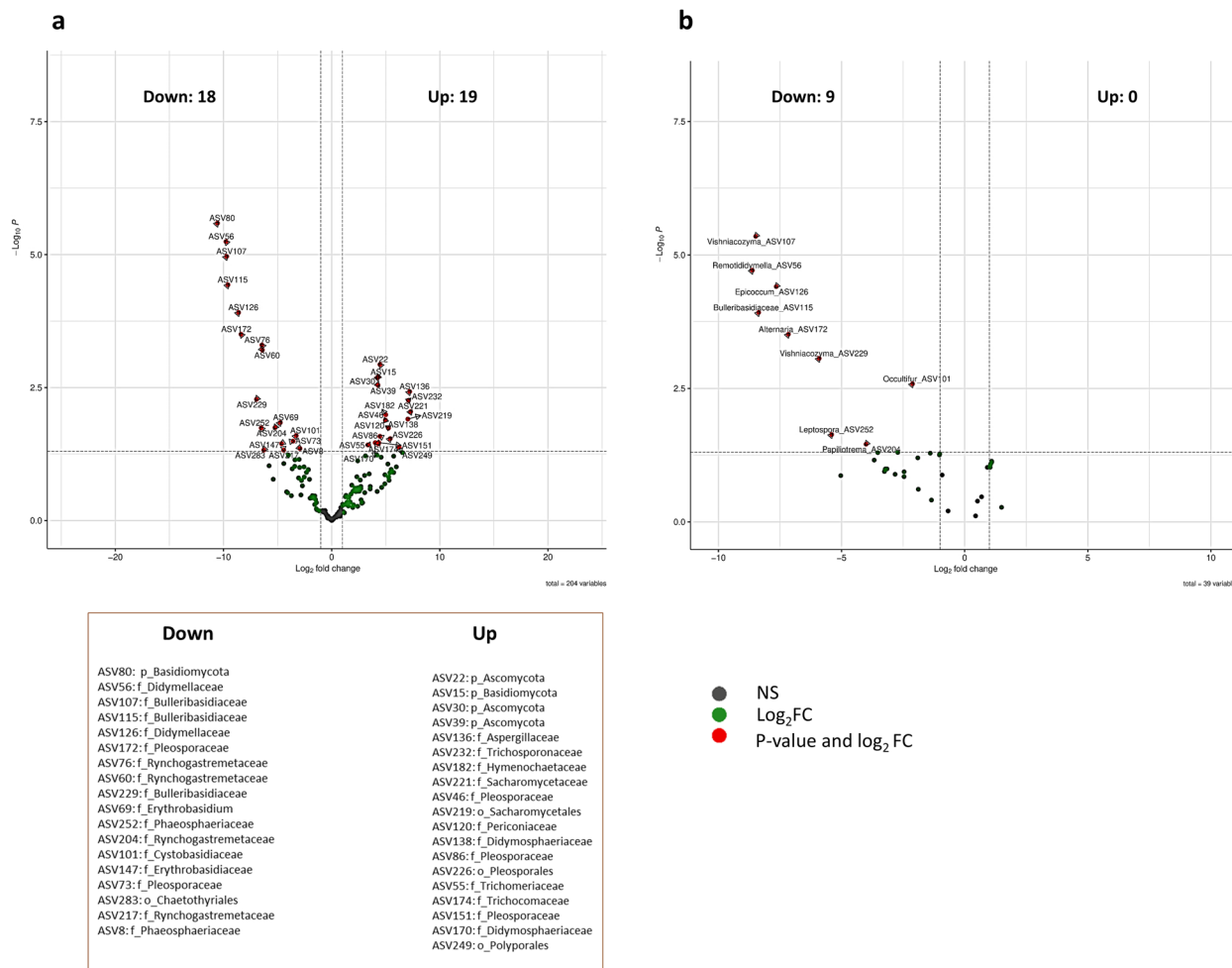


Fig. 4 Volcano plot representing the significantly enriched and depleted **a** fungal families and **b** fungal genera in the asymptomatic group compared to the symptomatic group. Each point on the graph represents a fungal family or genus. ASVs with a log₂ fold change ≥ 2 and p ≤ 0.05 are considered significantly enriched, while ASVs with a log₂ fold change ≤ -2 and p ≤ 0.05 are considered significantly depleted in the asymptomatic samples. Fungal families or genera with significantly different abundances lie above the horizontal threshold and are represented as red dots. Padj, adjusted p value. NS, not significant; FC, fold change

group (Fig. 8). The abundance of Pleosporaceae was significantly greater in the symptomatic group than in the asymptomatic group. *Alternaria* and *Curvularia* were the only two fungal genera identified in both culture-based and NGS-based studies. *Alternaria* was substantially more abundant in the symptomatic group than in the asymptomatic group.

Discussion

Fungal symbionts, including endophytes, help plants perform better by optimizing nutrient absorption and usage, boosting resistance to abiotic and biotic challenges, and

thereby enhancing plant development and health (Christian et al. 2017; Strobel 2018; Trivedi et al. 2020). Because of their beneficial effects on combating plant pathogens, the associated microbiota is often considered as an extended immune system in plants (Vannier et al. 2019). The invasion of phytopathogens causes changes in the composition and relationships of the internal microbial inhabitants and impacts the behavior of plant pathogens, thereby modulating disease dynamics (Zhang et al. 2018; Li et al. 2019; Luo et al. 2019; Akram et al. 2023). Advent of modern genomic technologies has greatly enhanced our ability to understand the changes in the phyllosphere

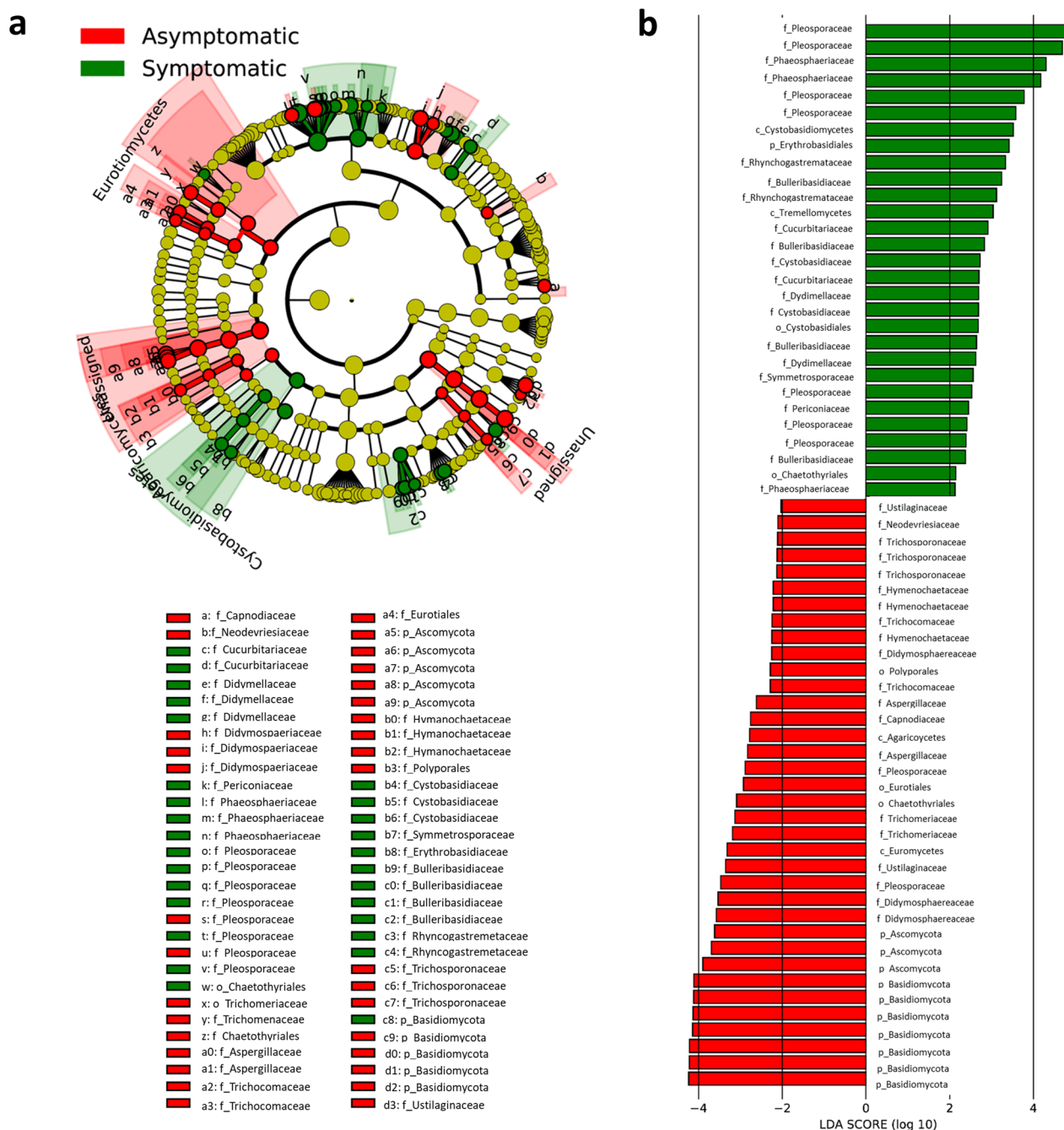


Fig. 5 a Cladogram and b LDA bar plot based on LEfSe analysis showing the taxa with significant differences between the asymptomatic and symptomatic groups for all the taxonomically assigned ASVs. Taxonomic hierarchies were arranged from the inside (lower taxonomic level) to the outside (higher taxonomic level). Red and green nodes in the phylogenetic tree represent differentially abundant taxa in the two groups. Yellow nodes represent taxa with no significant difference. In the bar plot, the horizontal bars represent the effect size for each taxon. The length of the bar represents the LDA score. Taxa with significant differences for ASVs with an LDA score $[\log_{10}] > 2$; p -value < 0.05 , FD adjusted. Letters in front of taxa represent taxonomic level (p =phylum, c =class, o =order, f =family)

microbiome and its effect on the ecosystem functioning in a changing environment (Zhu et al. 2022; Sohrabi et al. 2023). Identification and functional analysis of the microbial community members is a prerequisite for

constituting rationally designed synthetic communities (SynComs) that can potentially antagonize the pathogen attack (Pradhan et al. 2022). Deploying SynComs to enhance disease resistance is particularly relevant in the

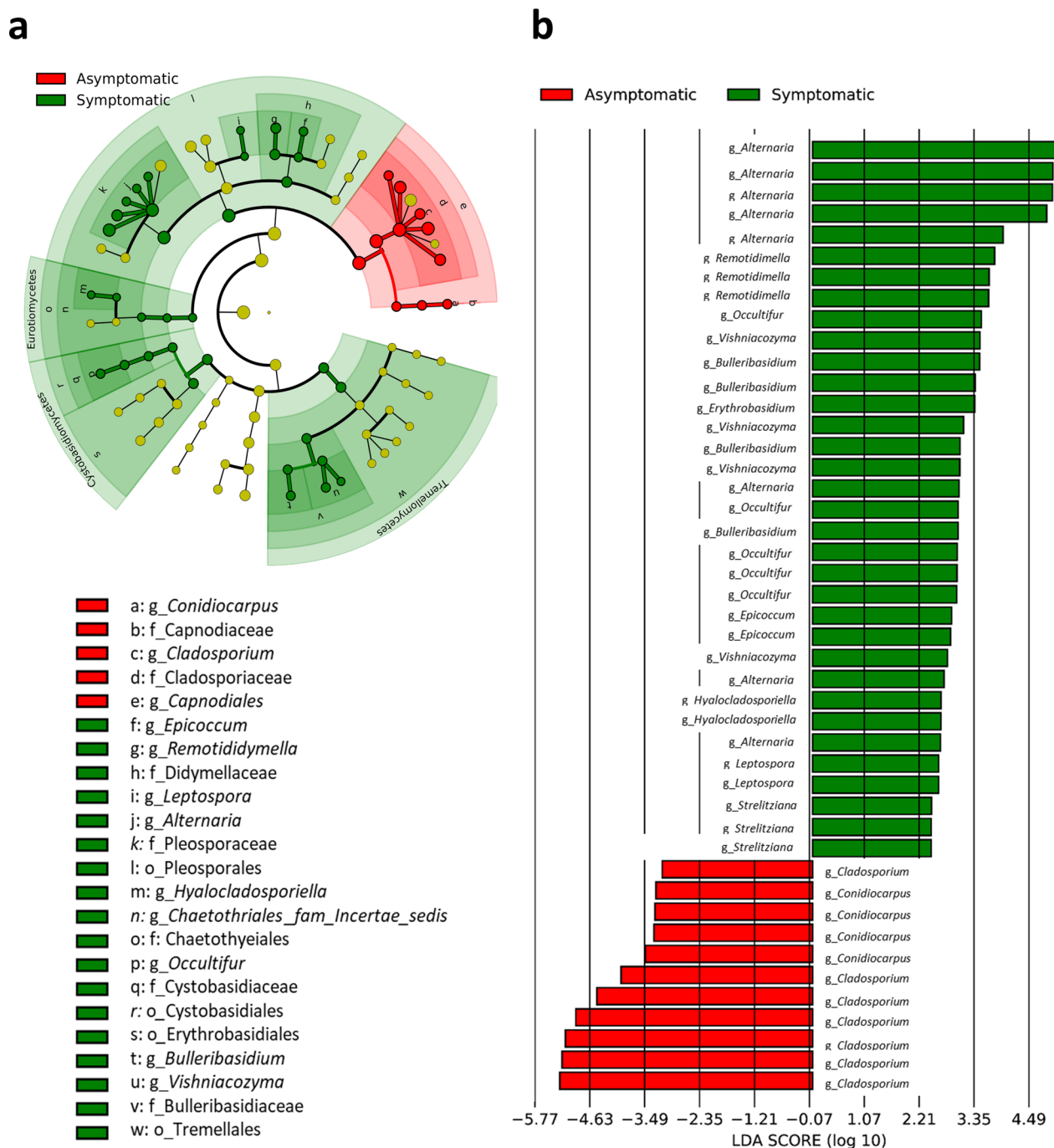


Fig. 6 a Cladogram and b LDA bar plot, based on LEfSe analysis showing the genera with significant differences between the asymptomatic and symptomatic groups. Taxonomic hierarchies were arranged from the inside (lower taxonomic level) to the outside (higher taxonomic level). Red and green nodes in the phylogenetic tree represent differentially abundant taxa in the two groups. Yellow nodes represent taxa with no significant difference. In the bar plot, the horizontal bars represent the effect size for each taxon. The length of the bar represents the LDA score. Taxa with significant differences for ASVs with an LDA score $[\log_{10}] > 2$; p -value < 0.05 , FD adjusted. The letters in front of the taxa represent the taxonomic level (g = genus)

context of cultivars that have limited scope of genetic improvement and plant species that are critically endangered (Zahn and Amend 2017).

Our study aimed to understand the diversity and trophic mode distribution of the fungal community associated with leaf spot disease in eggplant, focusing on the

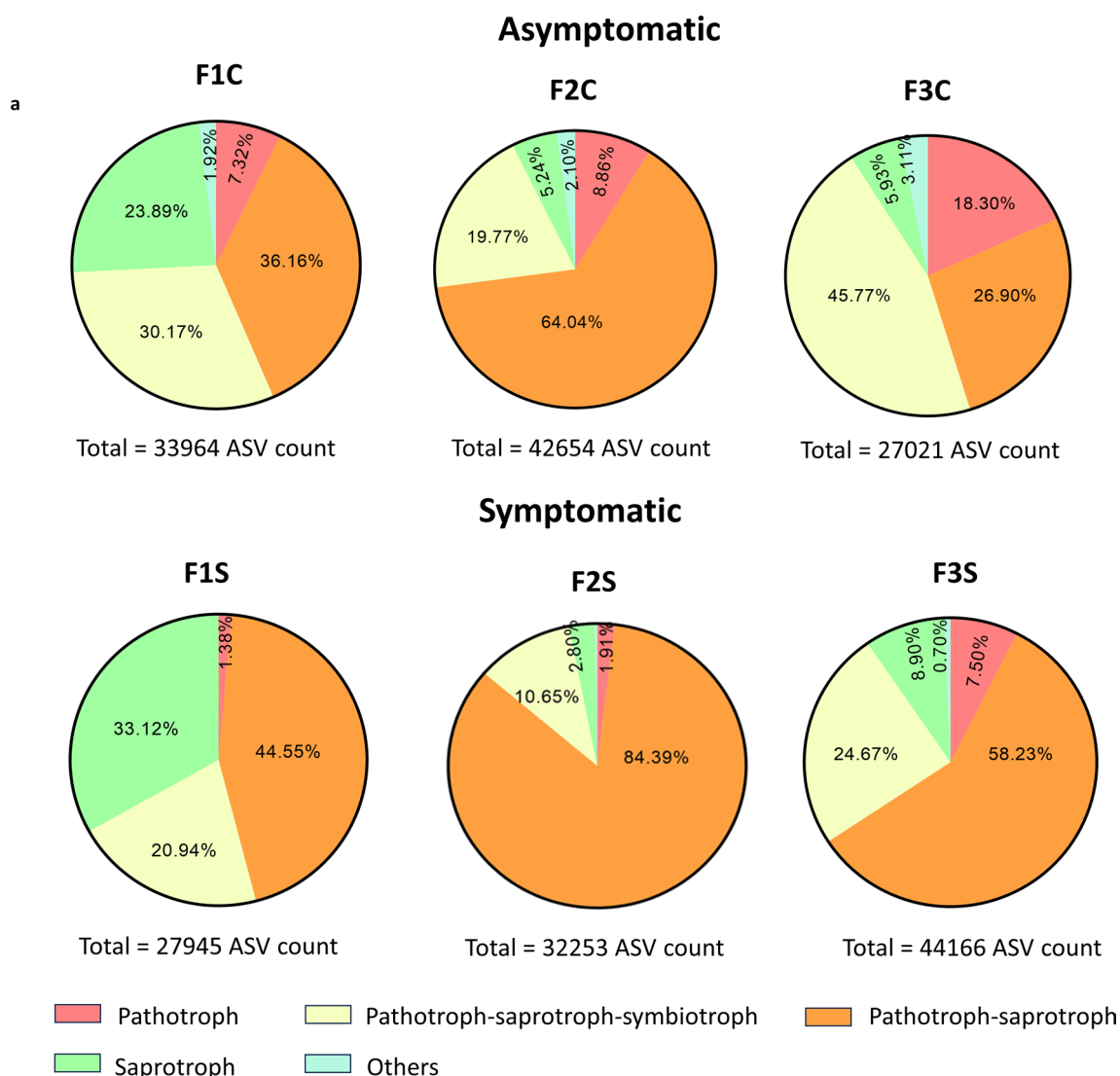


Fig. 7 Pie charts depicting the trophic mode distribution of the samples. Seven trophic modes were assigned using the FUNGuild tool. Pathotroph, Pathotroph-saprotroph, Pathotroph-saprotroph-symbiotroph, Saprotroph, and Others (includes Pathotroph-symbiotroph, Saprotroph-symbiotroph, and Symbiotroph). **a** asymptomatic group, **b** symptomatic group. F1C, F2C, and F3C represented asymptomatic group from field locations 1, 2, and 3, respectively; F1S, F2S, and F3S represented symptomatic group from field locations 1, 2, and 3, respectively

variety Mattu Gulla, which is a reputed traditional variety in the southern state of Karnataka in India that possesses a Geographical Indication (GI) tag. We followed traditional culturing and NGS-based ITS rRNA metabarcoding approaches to compare and elucidate the microbiome associated with symptomatic and asymptomatic leaf samples. Asymptomatic and symptomatic (with leaf spot symptoms) samples were collected and culturable fungi were isolated and identified using molecular biological methods. Fungal composition and distribution, richness and diversity, differential abundance, and trophic modes were elucidated in symptomatic and asymptomatic

groups in the present study. Finally, we compared the results from culture-based methods and metabarcoding approaches to understand the fungal community dynamics in leaf spot-affected conditions.

The disease-induced changes in the structure and variations of the fungal community in eggplant is poorly understood. Although attempts have been made previously to identify the leaf-spot-associated fungi in eggplant, the outcome was largely limited since it was solely dependent on a culture-based isolation strategy that leaves out a large proportion of unculturable species (Jinal et al. 2021). By combining culture-based and

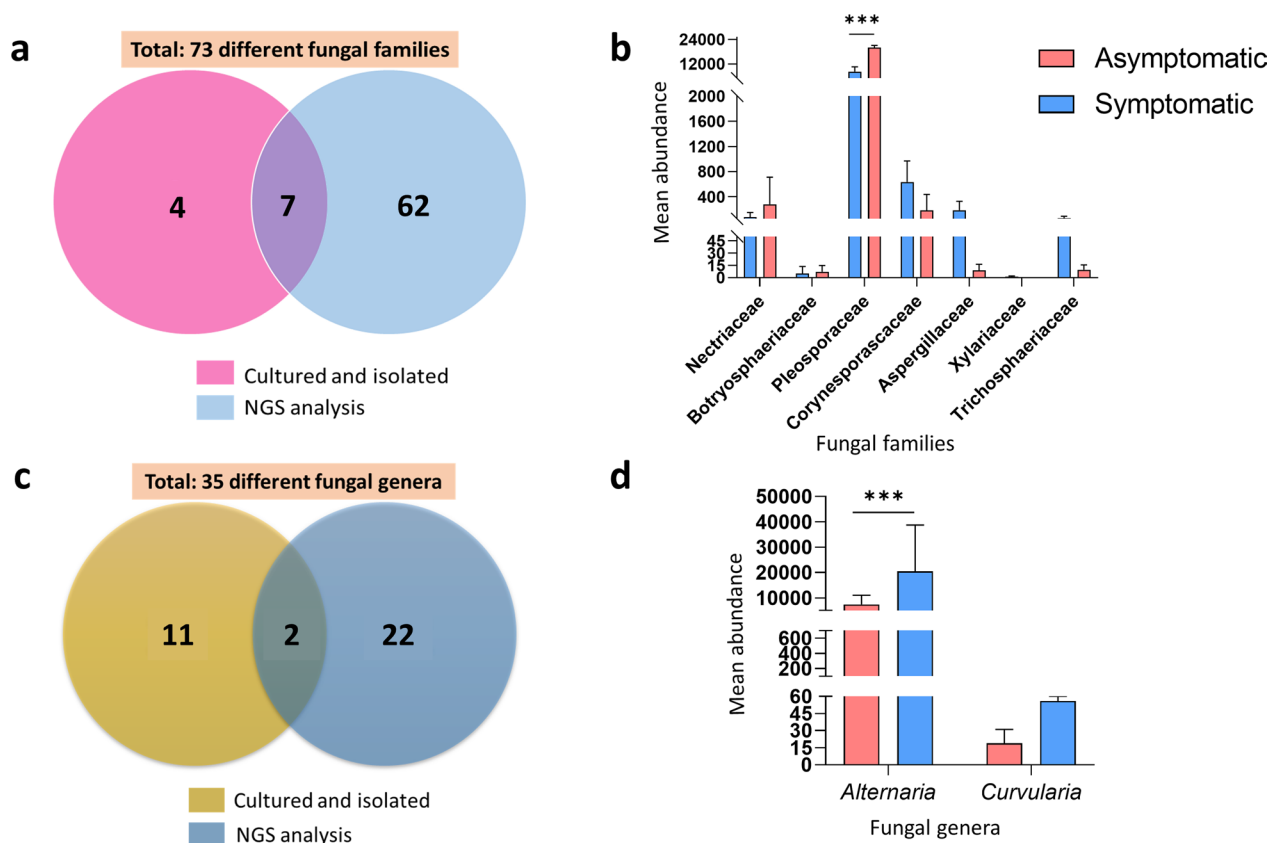


Fig. 8 a, c Venn diagrams representing the unique and common fungal families and genera identified using isolation and culturing methods and NGS analysis in both the symptomatic and asymptomatic groups. b, d Bar graphs represent the mean abundance of those commonly detected families and genera in the asymptomatic and symptomatic groups. *** represents $p \leq 0.001$

NGS-based methods, our study provides a more comprehensive understanding of the fungal diversity associated with eggplant. It is well established that fungi belonging to the phyla Ascomycota and Basidiomycota constitute a vast majority of the fungi that colonize plant tissues (Trivedi et al. 2020). Consistently, most of the fungal genera identified in our study from both asymptomatic and symptomatic groups belonged to these two phyla. The isolates associated with leaf spot of solanaceous crops, identified by Jinal et al. (2021) predominantly belonged to genera such as *Alternaria*, *Sarocladium*, *Nigrospora*, *Corynespora*, *Chaetomium*, *Penicillium*, and *Fusarium*. This list shows a remarkable overlap with the genera that we could isolate and identify by culture-based method (Additional file 2: Table S1). However, the differential abundance analysis from the NGS-based amplicon sequencing data suggested that *Alternaria*, *Remotididymella*, *Vishniacozyma*, *Bulleribasidium*, *Occultifur*, *Epicoccum*, and *Loratospora* are the abundant genera in the symptomatic leaves. Both culture-based and NGS-based methods expectedly showed *Alternaria*, a major leaf-spot-causing pathogen, as a predominant genus in

the symptomatic group. However, the large differences observed among the other abundant genera described by the two methods further highlight the potential limitation of the culture-based method in providing a holistic picture of the microbiome as compared with the metabarcoding approaches. Wang et al. (2022) reported that Ascomycota, Basidiomycota, and Glomeromycota are major phyla associated with walnut leaf spot disease, while Ascomycota and Basidiomycota were found to be dominant in angular leaf-spot of cucumber (Luo et al. 2019), which is comparable to our results.

The most abundant genus found in the asymptomatic leaves was *Cladosporium* (Fig. 6), a genus that includes pathogenic fungi causing foliar diseases as well as endophytic and phylloplane fungi (Bensch et al. 2012). The beneficial endophytes in the genus can produce plant-growth promoting compounds and metabolites against pathogenic fungi (Hamayun et al. 2010; Wang et al. 2013; R ut et al. 2021). The importance of profiling and understanding the pathogen-induced changes in the microbiome of plants has been well established in recent years (Trivedi et al. 2020; Pereira et al. 2023). Recruitment or

replacement of specific microorganisms as a strategy to combat diseases essentially reconstitutes the existing microbiome composition in plants (Liu et al. 2020). In general, the changes in the microbiome induced by fungal pathogens have been studied with a predominant focus on the bacterial microbiome on both the surface and endospheric regions of the leaf and root (Trivedi et al. 2020). Interestingly, as compared to bacterial communities, fungal communities have been reported to undergo a greater extent of changes in the presence of pathogens (Gao et al. 2021).

Contrasting observations exist on the effect of pathogen infection on the richness and diversity of plant fungal microbiome. According to our data, symptomatic leaves showed an increase in the richness and diversity of the fungal community as compared with the asymptomatic leaves (Fig. 2 and Additional file 1: Figure S2). Luo et al. (2019) reported an increase in fungal richness with an increase in the incidence of angular leafspot in cucumber. Dynamic changes in the foliar fungal community have been observed during different phases of disease progression in multiple cases, where the diversity and richness showed an initial increase, followed by a decrease (Zhang et al. 2018; Tao et al. 2021). No significant variation in the alpha or beta diversity of fungi was observed between healthy and greasy spot disease-infected citrus leaves (Abdelfattah et al. 2017). Despite showing no significant difference in alpha and beta diversity, our data indicated a considerable change in the fungal community structure following the incidence of leaf spot disease. This change was marked by an increase in both the abundance and diversity of the mycobiome (Fig. 1). The diversity of fungal microbiome showed an increase during *Fusarium* wilt in *Capsicum annuum*, whereas it showed a decrease in the case of *Fusarium* infection in tomato (Gao et al. 2021; Zhou et al. 2021). The effect of pathogens on mycobiome can also vary between different plant parts. It has been shown that the reproductive parts are less prone to pathogen-induced changes in their mycobiome as compared with the vegetative parts (Gao et al. 2021). Together, the dynamics and consequences of pathogen-microbiome interactions are context-dependent and may vary according to the genotype of the host plant (Busby et al. 2016; Laforest-Lapointe et al. 2016; Xiong et al. 2021). Along with the host factors, environmental factors such as temperature, pH, and precipitation contribute to regulating the microbial composition (Tedersoo et al. 2014; Cui et al. 2019; Větrovský et al. 2019; Gao et al. 2020; Faticov et al. 2021; Yan et al. 2022). These studies report diverging observations that suggest a highly varying influence of key environmental factors on determining the community structure (Huang et al. 2023). The lack of universality in the nature of the interactions between the host, the

environmental factors, and the microbiome composition highlights the necessity of specific investigations on various species and cultivars growing in different agro-climatic conditions.

Pathotroph-saprotroph was the predominant trophic mode in the symptomatic group, followed by pathotroph-saprotroph-symbiotroph and saprotroph modes (Fig. 7). The disturbances caused to the plant defense system and the partial tissue necrosis due to pathogen invasion may favor the fungi with pathotroph-saprotroph mode of nutrition. The symbiotrophic mode has been found to be very rare in the fungal community in both symptomatic and asymptomatic leaves. In general, the pathotroph and pathotroph-saprotroph-symbiotroph modes showed a decrease, whereas saprotrophic mode showed an increase in the symptomatic group as compared with the asymptomatic group. Saprotrophs play a critical role in the decomposition of organisms and the cycling of energy and nutrients and are the primary decomposers of dead or weak tissues (Promputtha et al. 2007). The field-to-field variations we could observe in our findings suggest that fungal community dynamics may differ based on shifts in associated environmental conditions.

Identification of specific fungal families and genera linked to diseases enables the exploration of microbial consortia to yield inoculants that enhance plant defense. This in turn facilitates breeding for resistant varieties and signals opportunities for precision disease management, including customized fungicides or biocontrol agents (Ali et al. 2023). Insights into broader ecological consequences can guide sustainable agriculture practices, reducing the application of chemicals (Liu et al. 2024). The unique GI status of eggplant var. Mattu Gulla underlines the importance of comparative analyses of fungal communities across regions for formulating tailor-made management strategies. Delineating the species-level composition of the fungal community structure is essential for further understanding the relative abundance of pathogenic, neutral, and beneficial fungi in diseased tissues. How the differentially enriched microbiota mechanistically contributes to direct microbial competition and disease dynamics also needs to be investigated further.

Understanding the changes induced in the physiological attributes of the eggplant by the alterations in the fungal microbiome is another important direction of study in the future. Studying the spatiotemporal changes in the microbiome and the host physiology in response to the disease will throw light on the possibility of systemically induced susceptibility in the host, where gradual changes in the metabolic pathways in the tissues lead to a spatially expanding suppression of the immune system in the host (Seybold et al. 2020). Studying genetic variations within fungal species will help identify markers

associated with pathogenicity and understand how these organisms evolve to overcome host defense. This can provide crucial information on the diverse mechanisms driving their virulence and adaptation (Satam et al. 2023). Our findings contribute significantly to understanding fungal community dynamics during disease conditions in eggplant. By identifying the fungal genera that undergo differential decline and enrichment in healthy and diseased leaves, our study sheds light on potential avenues for disease control through microecological management strategies. Moreover, our study points towards the scope of multidisciplinary approaches in unraveling the underlying mechanisms of microbiome responses to global changes. For example, integrating climate science with environmental microbiology holds promise for elucidating how seasonal shifts in temperature, precipitation, and other atmospheric parameters influence the structure and function of phyllosphere microbiomes. Furthermore, delving into the chemical ecology of the phyllosphere may offer valuable insights into microbiome-mediated processes such as nutrient cycling and biocontrol, and how these processes interplay with plant defense mechanisms during pathogen infection.

Conclusion

In summary, our study highlights the dynamics of leaf fungal microbiome during leaf spot disease in the host plant, with a specific focus on the eggplant variety Mattu Gulla. By employing a combination of traditional culturing methods and next-generation sequencing (NGS), we offer insights into the leaf-associated fungal community during symptomatic and asymptomatic conditions. Our investigation revealed distinct alterations in fungal community structure and trophic modes corresponding to the plant's health status, notably observing higher species richness in the leaf spot-infected group compared with the asymptomatic group. Our findings contribute significantly to understanding fungal community dynamics during disease conditions in eggplant, shedding light on potential avenues for disease control through microecological management strategies.

Methods

Ethics statement

The samples for this study were collected from private farmlands with the permission of the farmers of interest, who are Mattu Gulla Growers Association members at Mattu Village, Udupi, India. The members are acknowledged for their help and contribution, and the study did not involve any protected or endangered species.

Sampling and isolation of culturable fungi

The Mattu Gulla growing areas extend to longitudes of 74°43' 00"–74°46' 00" and latitudes of 13°13' 00"–13°15' 00", which are approximately 300 m away from the western coast (Arabian Sea). Sampling was conducted during 2018–2019 and 2019–2020. Five field locations were selected for the study based on geographical location and cropping pattern and were visited at regular intervals for observation and sample collection for the isolation of fungi. Typical leaf spot symptoms included defined margins and brown centers with concentric rings that eventually merged. During every visit, leaf samples were randomly collected in triplicate from each field location and brought to the laboratory. Immediately, the samples were processed to reduce the chance of other contaminants. The samples were surface sterilized according to Omar et al. (2023), and after surface sterilization, diseased tissue along with a small portion of the healthy area was cut into 5*5 mm sections and inoculated onto potato dextrose agar (PDA; SRL diagnostics, India) plates supplemented with 0.5 µg/mL chloramphenicol to inhibit bacterial growth. The plates were incubated at 27 ± 1°C for 3 to 4 days until mycelium development was observed. Morphologically, different isolates were identified and subjected to subculture, and different fungi were cultured and identified via morphological and molecular biological methods.

Morphological and molecular characterization of culturable fungi

The fungal isolates were cultured on potato dextrose agar at 27 ± 1°C for 10 days. The slide culture method was implemented to identify the isolates based on morphological features (Barman and Tamuli 2017). Mycelium was inoculated on a small piece of agar plug kept on a sterile glass slide. This was covered with a sterile coverslip and incubated on Whatman filter paper wetted with autoclaved distilled water inside a sterile petri plate. The whole setup was incubated for 7 days at 27 ± 1°C. The spores were stained using lactophenol cotton blue stain and observed under 40× magnification (Olympus PX5, Japan). For molecular identification, approximately 40 to 50 mg (wet weight) of fungal mycelium was collected, and genomic DNA was isolated using the NucleoSpin® Microbial DNA Kit by Macherey-Nagel with MN Beads Type C with mycelium disruption for 12 min following the protocol recommended by the manufacturer. The isolated DNA was electrophorized on a 0.8% agarose gel, followed by purity checking with a Nanodrop spectrophotometer (Eppendorf, India).

Amplification of the ITS rRNA gene

The ITS rRNA gene was amplified using the universal primers ITS1F (5'-TCCGTAGGTGAACCTGCGG-3') and ITS4R (5'-TCCTCCGCTTATTGATATGC-3') (White et al. 1990). PCR amplification was performed using a Mastercycler nexus gradient thermocycler (Eppendorf, India). A total reaction volume of 20 μ L containing 50 ng of DNA template was prepared using 2 \times PCR Mastermix (Maxome Labsciences, India), and the thermal cycling conditions were set as follows: initial denaturation at 95°C for 5 min; followed by 40 cycles at 95°C for 30 s, 52.5°C for 1 min, 72°C for 1 min; and a final extension at 72°C for 10 min. The amplified products were checked in a 1.8% agarose (w/v) gel and visualized under a gel documentation system (GENAXY Scientific Pvt. Ltd.). The amplified PCR products were purified using a QIAquick PCR Purification Kit (Qiagen, India). The purified PCR amplicons were further sequenced using specific ITS primers in a sequencer (Applied Biosystems® 3130 GA; Thermo Fisher Scientific, India). Sequences were identified using Basic Local Alignment Search Tool (BLAST) at the National Center for Biotechnology Information (NCBI) (<http://blast.ncbi.nlm.nih.gov/Blast.cgi>), with a cutoff score \geq 97%, and sequences were deposited in the GenBank under BioProject ID: PRJNA1029336.

Study site description and sample collection for NGS

Asymptomatic and symptomatic leaf samples were collected from the fields in Mattu Village, Udipi District, Karnataka, India, to analyze the fungal microbiome using a next-generation ITS rRNA-based metabarcoding approach. Three biological replicates were collected from three different field locations consisting of multiple nearby plots (GPS coordinates: Field 1, 13°16'18.2"N 74°44'10.4"E, Field 2, 13°27'40.1"N, 74°73'43.9"E, Field 3, 13°16'20.3"N, 74°43'38.2"E). Each field location is mentioned as samples F1, F2, and F3, respectively, while from each field, three different plots were considered for sample collection. From each plot, leaf samples (symptomatic and asymptomatic) were collected in triplicate so that the sampling consisted of a pool of nine samples and a total of 27 samples representing asymptomatic and symptomatic groups, respectively (Additional file 1: Figure S4). The field location was selected so that they represented nearby and far-away localities to the river and sea, ensuring a varied geographical distribution within the limited cultivation area. The uniformity of agricultural practices and plant age were also considered when choosing the field location. Infected leaves that showed a disease lesion to a minimum severity grade of 5 (12 to 25% leaf area affected) according to the Horsfall and Baratt (H–B) grade scale (Chiang et al. 2020; Guan et al.

2023) were collected only to maintain uniformity. H–B is a semiquantitative scale for the visual assessment of plant disease. After collection, the leaf samples were wiped with 70% ethanol and freeze-dried using liquid nitrogen until further processing for NGS. One part of the disease-affected leaf tissue was used to isolate culturable microfungi.

Genomic DNA extraction for NGS

Among the pooled samples, three replicates were used for DNA extraction. Genomic DNA was isolated using the HiPurA® Plant Genomic DNA Miniprep Purification Kit (HiMedia laboratories, MB507) following the manufacturer's instructions. All samples were subjected to a quality check using a spectrophotometer. The concentration of the DNA samples was $>$ 50 ng/ μ L and an A260/280 ratio close to 1.8 and a 260/230 ratio $>$ 2.0. For validation of the template quality, general PCR targeting the ITS region was performed for each sample to check the amplification at two concentrations of template DNA in the reaction (1 ng/ μ L and 5 ng/ μ L). The success rate of DNA amplification was around 95%. Only the PCR-successful samples were taken for further processing.

Illumina library preparation and sequencing

The PCR-successful samples were quantified with a Qubit fluorometer using a dsDNA broad-range kit (Thermo Fisher Scientific). The samples were then diluted to 1 ng/ μ L in low Tris- Ethylenediaminetetraacetic acid (TE) buffer and subjected to a library preparation workflow for the ITS region using the Illumina demonstrated protocol for ITS sequencing with a phased primer strategy. The protocol uses a phased primer approach outlined by Fadrosh et al. (2014). Indexed libraries were purified and pooled at equimolar concentrations to a concentration of 10 nM. The pool was further validated using an Agilent Tape station 4200 high-sensitivity D1000 screentape (Agilent) and quantified using a high-sensitivity ds DNA kit (Thermo Fisher Scientific) from a qubit fluorometer. The pooled library was run in duplicate on an Illumina MiSeq instrument using the 2 \times 250 base chemistry of the v2 reagent kit according to the manufacturer's instructions (HiMedia laboratories Pvt. Ltd., Mumbai, India). The reads produced were demultiplexed on board the sequencer, and raw fastq files were generated.

Sequence quality assessment

An initial assessment of the raw FASTQ files was carried out using the software FastQC v0.11.9 (Andrews 2010). The quality of the sequences used for downstream processing is depicted in Additional file 1: Figure S5. The parameters used to check the raw data quality were, as reported by Ewels et al. (2016), used to determine the

quantity of data obtained for each of the paired-read files for an individual sample. The fastp tool (v0.12.4) was used to remove adapter contamination (Chen et al. 2018). A quality score greater than or equal to Q30 shows that the basecall accuracy at that position is supported by a probability score of 99.9%. The resulting files for each amplicon were used as input for downstream processing.

Illumina sequence processing

Cleaning protocols were implemented within the software package to infer ITS variants, i.e., the DADA2 package (v3.11) (Callahan et al. 2016). Graphical profile of reads was generated in both forward and reverse read files to get a quality. Although our input data were prefiltered, in our workflow, we additionally used parameters prescribed by the DADA2 package (v3.11) (Callahan et al. 2016). After cleaning the reads, each sample's error profile was computed within DADA2 for both forward and reverse reads. The algorithm uses a machine learning approach to learn error rates by reconciling sample errors with a prior error model to reach a consensus. Once the error rates were determined for the entire sample set, the error model was separately applied to each forward and reverse read pair. The remaining read pairs were merged to prepare input for querying the database. In the next step, we removed chimeras from our data. As a final step, before querying the database, we collated the read statistics from each of the above steps. The codes used for processing are provided as Additional file 3.

OTU design and statistical analysis

A naive Bayesian classifier was used to assign taxonomy using available databases. Once completed, we proceeded with advanced microbial ecology-based analyses, which can be executed in the R package phyloseq (McMurdie and Holmes 2013). Diversity analyses of the microbiomes were plotted using the Plotly.js (v2.11.1) software package and Microbiome Analyst 2.0 (Lu et al. 2023) online software. Plotly.js was chosen because of its interactive visualization capabilities, allowing users to explore and manipulate the data dynamically, its ability to customize visual elements, clarity of the presented data, and compatibility with various programming languages, providing flexibility in implementation. Microbiome Analyst 5.0 is a user-friendly, comprehensive tool with updated references. Statistical meta-analysis was performed for microbiome analysis for diversity and abundance analysis. The low count filter score was set to 20% to remove features with a small count, and the minimum count off was set to 4. The low variance was measured using the interquartile range, with a percentage cutoff of 10%. Data normalization was performed using total sum scaling (TSS).

The significance of the diversity analysis was calculated using the Mann–Whitney U test (nonparametric test) ($p < 0.05$). The DESeq2 package in R was used to detect differentially abundant ASVs that may drive the differences observed between inferred microbial communities (Love et al. 2014). Differential abundance analysis was performed between asymptomatic and symptomatic sample data, and the ASVs with a \log_2 -fold change ≥ 2 and $p \leq 0.05$ were considered significantly enriched, while the ASVs with a \log_2 -fold change ≤ -2 and $p \leq 0.05$ were considered considerably depleted in the asymptomatic leaf samples. A \log_2 -fold change threshold of ≥ 2 was selected to focus on ASVs with a substantial change in abundance. The choice of a p value threshold of ≤ 0.05 is consistent with DESeq2's methodology and standard practices in statistical hypothesis testing. Linear discriminant analysis (LDA) using the effect size (LEfSe) method (Segata et al. 2011) with default parameters was used to examine intergroup differences at the phylum, class, order, family, and genus levels in each cluster (<https://huttenhower.sph.harvard.edu/galaxy/root>). To assess the importance of variations in ASVs between the two groups, LEfSe employs the two-tailed nonparametric Kruskal–Wallis test. Furthermore, the FUNGuild database was used to assign trophic modes to ASVs (Mertin et al. 2022; Yang et al. 2022). Prediction of the functional composition of the microbial community from its ITS profiles was carried out using the PICRUSt2 tool (Douglas et al. 2020) with default parameters.

Abbreviations

ASV	Amplicon sequence variants
BLAST	Basic local alignment search tool
DNA	Deoxyribonucleic acid
GI	Geographic indication
GPS	Global positioning system
H–B grade scale	Horsfall and Baratt grade scale
ITS	Internal transcribed spacer
LDA	Linear discriminant analysis score
LEfSe	Linear discriminant effect size
NCBI	National Center for Biotechnology Information
NGS	Next generation sequencing
NMDS	Nonmetric multidimensional scaling
PCoA	Principal coordinate analysis
PCR	Polymerase chain reaction
PDA	Potato dextrose agar
PICRUSt	Phylogenetic investigation of communities by reconstruction of unobserved states
rRNA	Ribosomal ribonucleic acid
TE	Tris-ethylenediaminetetraacetic acid
TSS	Total sum scaling

Supplementary Information

The online version contains supplementary material available at <https://doi.org/10.1186/s42483-024-00277-2>.

Supplementary Material 1: Figure S1. Macroscopic and microscopic characteristics of fungi isolated from the leaf spot of the eggplant Mattu Gulla. The upper surface of the fungi is shown in the top panels. a. AKMG1

to a. AKMG18. The microscopy images shown in panels b1 to b18 were taken at 40X with a scale of 20 μ m. **Figure S2.** The Rarefaction curve plot showing the species richness of the samples from the three different field locations studied. Samples 1 to 3 represented asymptomatic group from field locations 1, 2, and 3, respectively; Samples 4 to 6 represented symptomatic group from field locations 1, 2, and 3, respectively. **Figure S3.** Heatmap for the prediction of the top 30 MetaCyc pathways per category of functional composition of the microbial community metagenome from its ITS profiles. The data are presented as the relative abundance per sample for the symptomatic and asymptomatic groups. F1S, F2S, and F3S represented Symptomatic group samples from field locations 1, 2, and 3, respectively. **Figure S4.** Experimental design followed for the collection of leaf samples for microbiome profiling using NGS. Samples were collected from three fields at different locations. Three plots were considered from each field location. Triplicate sampling was performed from each plot with three symptomatic and three asymptomatic leaves. Asymptomatic and symptomatic leaves collected from each field location were separately pooled to obtain one sample for further analysis. **Figure S5.** Sequence quality histograms. **a** The mean quality value across each base position in the read. **b** The number of reads with average quality scores. **c** The percentage of base calls at each position for which an N was called.

Supplementary Material 2: Table S1. Identification of fungal isolates associated with leaf spot in *S. melongena* var. Mattu Gulla using ITS rRNA sequence analysis. **Table S2.** Sequence processing results from each step for the six samples. The sequences were filtered, denoised, and nonchimeric sequences were removed. The final processed sequences were considered for further analysis. F1C, F2C, and F3C represented asymptomatic groups from field locations 1, 2, and 3, respectively; F1S, F2S, and F3S represented symptomatic groups from field locations 1, 2, and 3, respectively. **Table S3.** The relative abundance of fungal phyla in asymptomatic and symptomatic groups from the individual field locations. F1C, F2C, and F3C represented asymptomatic group samples from field locations 1, 2, and 3, respectively; F1S, F2S, and F3S represented asymptomatic group samples from field locations 1, 2, and 3, respectively. **Table S4.** Richness estimators and diversity indices for the six samples. F1C, F2C, and F3C represented asymptomatic groups from field locations 1, 2, and 3, respectively; F1S, F2S, and F3S represented symptomatic groups from field locations 1, 2, and 3, respectively. **Table S5.** List of taxonomically assigned ASVs identified from the NGS analysis of asymptomatic and symptomatic samples collected from the three field locations. **Table S6.** Differential abundance analysis data for the ASVs belonging to the asymptomatic group along with the base mean, log₂-fold change, lfcSE, p value and padj values for each ASV.

Supplementary Material 3: The codes used for processing the Illumina sequences.

Acknowledgements

We thank the Manipal Academy of Higher Education (MAHE) and the Manipal School of Life Sciences, Manipal, Karnataka, India, and TIFAC-CORE and FIST, DST New Delhi, DBT-BUILDER grant (BT/INF/22/SP43065/2021) and K-FIST, VGST, Govt. of Karnataka for the infrastructure and facilities. The authors (AK and SAT) are grateful to the Manipal Academy of Higher Education (MAHE) for Dr. T.M.A. Pai PhD scholarship, and AK is thankful to the Indian Council of Medical Research (ICMR), Govt. of India for financial assistance as Project Associate-I through a research grant (No. 59/08/2022-TRM/BMS). The authors thank HiMedia Laboratories Pvt. Ltd., Mumbai, especially Mr. Gobinath S. for the experimental and analytical support. We thank Prof. B.S. Satish Rao, Director, Manipal School of Life Sciences, MAHE, for their constant encouragement. Special thanks to Dr. Vishnu Prasoodanan, Postdoctoral Fellow, Umeå University, Västerbotten, Sweden, for assistance in the data analysis. We also thank Mr. Pradhyumna Jayaram and Mr. Venkidesh B. S. Ms. Debyani S., PhD. Scholars, MSLS, MAHE for all their help. We would like to thank Mrs. Shashikala Tantry, Mrs. Usha R.N. and Mr. Raju N.D. for experimental assistance. The authors are greatly indebted to Mr. Mohan Rao, Mr. Lakshmana Rao, Mr. Lakshman Mattu and Mr. Vasu Poojari, Members of Mattu Gulla Growers Association, Mattu Village, Udupi District, Karnataka, India, for field access and plant samples. We are grateful to reviewers and editorial board members for their critical suggestions and comments to improve the earlier versions of the manuscript.

Author contributions

AM, AK, and TSM designed the study; AK, SAT, MRR, and AM performed the field survey and collected the samples. AK, SBS, and AM performed the experiments and analyzed the data; AK, SBS, and AM validated the data and wrote the manuscript; AK, SAT, AM, and TSM edited the manuscript; and all authors approved the final version for submission.

Funding

Not applicable.

Availability of data and materials

The authors confirm that the data and related information supporting the findings of this study are available within the article and its supplementary materials.

Declarations

Ethics approval and consent to participate

Not applicable.

Consent for publication

Not applicable.

Competing interests

The authors declare that they have no known competing financial interests or personal relationships that could have appeared to influence the work reported in this paper.

Received: 4 December 2023 Accepted: 14 August 2024

Published online: 05 November 2024

References

- Abdelfattah A, Cacciola SO, Mosca S, Zappia R, Schena L. Analysis of the fungal diversity in citrus leaves with greasy spot disease symptoms. *Microb Ecol.* 2017;73:739–49. <https://doi.org/10.1007/s00248-016-0874-x>.
- Agler MT, Ruhe J, Kroll S, Morhenn C, Kim ST, Weigel D, Kemen EM. Microbial hub taxa link host and abiotic factors to plant microbiome variation. *PLoS Biol.* 2016;14:e1002352. <https://doi.org/10.1371/journal.pbio.1002352>.
- Akram S, Ahmed A, He P, He P, Liu Y, Wu Y, He Y. Uniting the role of endophytic fungi against plant pathogens and their interaction. *J Fungi.* 2023;9:72. <https://doi.org/10.3390/jof9010072>.
- Ali S, Tyagi A, Bae H. Plant Microbiome: An Ocean of Possibilities for Improving Disease Resistance in plants. *Microorganisms.* 2023;11:392. <https://doi.org/10.3390/microorganisms11020392>.
- Andrews S. FastQC: a quality control tool for high throughput sequence data. 2010; <https://www.bioinformatics.babraham.ac.uk/projects/fastqc/>
- Aumentado HD, Balendres MA. Characterization of *Corynespora cassiicola* causing leaf spot and fruit rot in eggplant (*Solanum melongena* L.). *Arch Phytopathol Plant Prot.* 2022;55:1304–16. <https://doi.org/10.1080/03235408.2022.2091211>.
- Barman A, Tamuli R. The pleiotropic vegetative and sexual development phenotypes of *Neurospora Crassa* arise from double mutants of the calcium signaling genes *plc-1*, *splA2*, and *cpe-1*. *Curr Genet.* 2017;63:861–75. <https://doi.org/10.1007/s00294-017-0682-y>.
- Bensch K, Braun U, Groenewald JZ, Crous PW. The genus *cladosporium*. *Stud Mycol.* 2012;72:1–401. <https://doi.org/10.3114/sim0003>.
- Bhat RV, Madhyastha MN. Preserving the Heritage of Mattu Gulla. A Variety of Brinjal Unique to Udupi District. *Curr Sci.* 2007;93:905–6.
- Blackwell M. The Fungi: 1, 2, 3 ... million species? *Am J Bot.* 2011;98:426–38. <https://doi.org/10.3732/ajb.1000298>.
- Bringel F, Coué I. Pivotal roles of phyllosphere microorganisms at the interface between plant functioning and atmospheric trace gas dynamics. *Front Microbiol.* 2015;6:486. <https://doi.org/10.3389/fmicb.2015.00486>.
- Busby PE, Peay KG, Newcombe G. Common foliar fungi of *Populus trichocarpa* modify *Melampsora* rust disease severity. *New Phytol.* 2016;209:1681–92. <https://doi.org/10.1111/nph.13742>.

- Callahan BJ, McMurdie PJ, Rosen MJ, Han AW, Johnson AJA, Holmes SP. DADA2: high-resolution sample inference from Illumina amplicon data. *Nat Methods*. 2016;13:581–3. <https://doi.org/10.1038/nmeth.3869>.
- Carvalho SD, Castillo JA. Influence of light on plant–Phyllosphere Interaction. *Front Plant Sci*. 2018;9:1482. <https://doi.org/10.3389/fpls.2018.01482>.
- Chen S, Zhou Y, Chen Y, Gu J. Fastp: an ultrafast all-in-one FASTQ preprocessor. *Bioinformatics*. 2018;34:i884–90. <https://doi.org/10.1093/bioinformatics/bty560>.
- Chiang KS, Liu HI, Chen YL, El Jarroudi M, Bock CH. Quantitative ordinal scale estimates of plant disease severity: comparing treatments using a proportional odds model. *Phytopathology*. 2020;110:734–43. <https://doi.org/10.1094/PHYTO-10-18-0372-R>.
- Christian N, Herre EA, Mejia LC, Clay K. Exposure to the leaf litter microbiome of healthy adults protects seedlings from pathogen damage. *Proc R Soc B*. 2017;284:20170641. <https://doi.org/10.1098/rspb.2017.0641>.
- Cui Y, Bing H, Fang L, Wu Y, Yu J, Shen G, Jiang M, Wang X, Zhang X. Diversity patterns of the rhizosphere and bulk soil microbial communities along an altitudinal gradient in an alpine ecosystem of the eastern tibetan Plateau. *Geoderma*. 2019;338:118–27. <https://doi.org/10.1016/j.geoderma.2018.11.047>.
- Dastogeer KM, Yasuda M, Okazaki S. Microbiome and pathobiome analyses reveal changes in community structure by foliar pathogen infection in rice. *Front Microbiol*. 2022;13:949152. <https://doi.org/10.3389/fmicb.2022.949152>.
- De Vries FT, Griffiths RI, Bailey M, Craig H, Girlanda M, Gweon HS, Hallin S, Kaisermann A, Keith AM, Kretzschmar M, Lemanceau P, Lumini E, Mason KE, Oliver A, Ostle N, Prosser JI, Thion C, Thomson B, Bardgett, RD. Soil bacterial networks are less stable under drought than fungal networks. *Nat Commun*. 2018;9:3033. <https://doi.org/10.1038/s41467-018-05516-7>.
- Douglas GM, Maffei VJ, Zaneveld JR, Yurgel SN, Brown JR, Taylor CM, Langille MG. PICRUSt2 for prediction of metagenome functions. *Nat Biotechnol*. 2020;38:685–8. <https://doi.org/10.1038/s41587-020-0548-6>.
- Edwards J, Johnson C, Santos-Medellin C, Lurie E, Podishetty NK, Bhatnagar S, Eisen JA, Sundaresan V. Structure, Variation, and assembly of the root-associated microbiomes of rice. *Proc Natl Acad Sci*. 2015;112:E911–20. <https://doi.org/10.1073/pnas.1414592112>.
- Ewels P, Magnusson M, Lundin S, Käller M, MultiQC. Summarize analysis results for multiple tools and samples in a single report. *Bioinformatics*. 2016;32:3047–8. <https://doi.org/10.1093/bioinformatics/btw354>.
- Fadrosch DW, Ma B, Gajer P, Sengamalay N, Ott S, Brotman RM, Ravel J. An improved dual-indexing approach for multiplexed 16S rRNA gene sequencing on the Illumina MiSeq platform. *Microbiome*. 2014;2:6. <https://doi.org/10.1186/2049-2618-2-6>.
- Faticov M, Abdelfattah A, Roslin T, Vacher C, Hambäck P, Blanchet FG, Lindahl BD, Tack AJ. Climate warming dominates over plant genotype in shaping the seasonal trajectory of foliar fungal communities on oak. *New Phytol*. 2021;231:1770–83. <https://doi.org/10.1111/nph.17434>.
- Gao C, Montoya L, Xu L, Madera M, Hollingsworth J, Purdom E, Taylor JW. Fungal community assembly in drought-stressed sorghum shows stochasticity, selection, and universal ecological dynamics. *Nat Commun*. 2020;11:34. <https://doi.org/10.1038/s41467-019-13913-9>.
- Gao M, Xiong C, Gao C, Tsui CKM, Wang MM, Zhou X, Zhang AM, Cai L. Disease-induced changes in plant microbiome assembly and functional adaptation. *Microbiome*. 2021;9:187. <https://doi.org/10.1186/s40168-021-01138-2>.
- Ginnan NA, Dang T, Bodaghi S, Ruegger PM, Peacock BB, McCollum G, England G, Vidalakis G, Roper C, Rolshausen P, Borneman J. Phytobiomes J. Bacterial and fungal next generation sequencing datasets and metadata from citrus infected with "*Candidatus Liberibacter asiaticus*". *Phytobiomes J*. 2018;2:64–70. <https://doi.org/10.1094/PBIOMES-08-17-0032-A>.
- Guan W, Bonkowski J, Creswell T, Egel DS. Strawberry Cultivar susceptibility to Neopestalotiopsis leaf spot in Indiana. *Plant Health Prog*. 2023;24:135–9. <https://doi.org/10.1094/PHP-05-22-0049-RS>.
- Hacquard S, Schadt CW. Toward a holistic understanding of the beneficial interactions across the Populus microbiome. *New Phytol*. 2015;205:1424–30. <https://doi.org/10.1111/nph.13133>.
- Hamayun M, Khan SA, Khan AL, Rehman G, Kim YH, Iqbal I, Lee JJ. Gibberellin production and plant growth promotion from pure cultures of *Cladosporium* sp. MH-6 isolated from cucumber (*Cucumis sativus* L.). *Mycologia*. 2010;102:989–95. <https://doi.org/10.3852/09-261>.
- Huang S, Zha X, Fu G. Affecting factors of plant phyllosphere microbial community and their responses to climatic warming—A review. *Plants*. 2023;12:2891. <https://doi.org/10.3390/plants12162891>.
- Jinal HN, Vibhuti M, Amaran N. Isolation and pathogenicity of leaf-spot-associated fungi isolated from solanaceous crops grown in South Gujarat, India. *Natl Acad Sci Lett*. 2021;44:351–3. <https://doi.org/10.1007/s40009-020-01024-9>.
- Kaniyassery A, Thorat SA, Kiran KR, Murali TS, Muthusamy A. Fungal diseases of eggplant (*Solanum melongena* L.) and components of the disease triangle: a review. *J Crop Improv*. 2023;37:1–52. <https://doi.org/10.1080/15427528.2022.2120145>.
- Kaniyassery A, Hegde M, Sathish SB, Thorat SA, Udupa S, Murali TS, Muthusamy A. Leaf spot-associated pathogenic fungi alter photosynthetic, biochemical, and metabolic responses in eggplant during the early stages of infection. *Physiol Mol Plant Pathol*. 2024;133:102320. <https://doi.org/10.1016/j.pmpp.2024.102320>.
- Krstić Tomić T, Atanasković I, Nikolić I, Joković N, Stević T, Stanković S, Lozo J. Culture-dependent and metabarcoding characterization of the sugar beet (*Beta vulgaris* L.) microbiome for high-yield isolation of bacteria with plant growth-promoting traits. *Microorganisms*. 2023;11:1538. <https://doi.org/10.3390/microorganisms111061538>.
- Laforest-Lapointe I, Messier C, Kembel SW. Host species identity, site and time drive temperate tree phyllosphere bacterial community structure. *Microbiome*. 2016;4:27. <https://doi.org/10.1186/s40168-016-0174-1>.
- Li M, Wei Z, Wang J, Jousset A, Friman V, Xu Y, Shen Q, Pommier T. Facilitation promotes invasions in plant-associated microbial communities. *Ecol Lett*. 2019;22:149–58. <https://doi.org/10.1111/ele.13177>.
- Liu H, Brettell LE, Qiu Z, Singh BK. Microbiome-mediated stress resistance in plants. *Trends Plant Sci*. 2020;25:733–43. <https://doi.org/10.1016/j.tplants.2020.03.014>.
- Liu S, Guo N, Jin J, Zhang Q, Yu Y. (2024). Characterizing the alterations in the Phyllosphere Microbiome in Relation to Blister Blight Disease in Tea plants. 16 January 2024, PREPRINT (Version 1) available at Research Square.
- Love MI, Huber W, Anders S. Moderated estimation of Fold change and dispersion for RNA-seq data with DESeq2. *Genome Biol*. 2014;15:550. <https://doi.org/10.1186/s13059-014-0550-8>.
- Lu Y, Zhou G, Ewald J, Pang Z, Shiri T, Xia J. MicrobiomeAnalyst 2.0: comprehensive statistical, functional and integrative analysis of microbiome data. *Nucleic Acids Res*. 2023;51:W310. <https://doi.org/10.1093/nar/gkad407>.
- Lundberg DS, Lebeis SL, Paredes SH, Yourstone S, Gehring J, Malfatti S, Tremblay J, Engelbrekton A, Kunin V, Rio TGD, Edgar RC, Eickhorst T, Ley RE, Hugenholtz P, Tringe S, Dangl JL. Defining the core *Arabidopsis thaliana* root microbiome. *Nature*. 2012;488:86–90. <https://doi.org/10.1038/nature1237>.
- Luo L, Zhang Z, Wang P, Han Y, Jin D, Su P, Tan X, Zhang D, Muhammad-Rizwan H, Lu X, Liu Y. Variations in phyllosphere microbial community along with the development of angular leaf-spot of cucumber. *AMB Express*. 2019;9:76. <https://doi.org/10.1186/s13568-019-0800-y>.
- McMurdie PJ, Holmes S. Phyloseq: an R Package for Reproducible Interactive Analysis and Graphics of Microbiome Census Data. *PLoS ONE*. 2013;8:e61217. <https://doi.org/10.1371/journal.pone.0061217>.
- Mehrotra S, Mishra S, Srivastava V. Plant–Pathogen interactions studies: Combinatorial Approach and Multidisciplinary benefits. *Plant Pathogen Interaction*. Singapore: Springer Nature Singapore; 2024. pp. 3–9. https://doi.org/10.1007/978-981-99-4890-1_1.
- Mertin AA, Laurence MH, Van Der Merwe M, French K, Liew ECY. The culturable seed mycobiome of two *Banksia* species is dominated by latent saprotrophic and multitrophic fungi. *Fungal Biol*. 2022;26:738–45. <https://doi.org/10.1016/j.funbio.2022.09.002>.
- Omar NH, Mohd M, Mohamed Nor NMI, Zakaria L. Characterization and pathogenicity of *Fusarium* species associated with leaf spot of mango (*Mangifera indica* L.). *Microb Pathog*. 2023;114:362–8. <https://doi.org/10.1016/j.micpath.2017.12.026>.
- Pereira LB, Thomazella DP, Teixeira PJ. Plant-microbiome crosstalk and disease development. *Curr Opin Plant Biol*. 2023;72:102351. <https://doi.org/10.1016/j.pbi.2023.102351>.
- Pradhan S, Tyagi R, Sharma S. Combating biotic stresses in plants by synthetic microbial communities: principles, applications and challenges. *J Appl Microbiol*. 2022;133:5:2742–59. <https://doi.org/10.1111/jam.15799>.

- Promptuttha I, Lumyong S, Dhanasekaran V, McKenzie EHC, Hyde KD, Jeewon R. A phylogenetic evaluation of whether endophytes become saprotrophs at host senescence. *Microb Ecolo.* 2007;53:579–90. <https://doi.org/10.1007/s00248-006-9117-x>.
- Răut I, Călin M, Capră L, Gurban AM, Doni M, Radu N, Jecu L. *Cladosporium* sp. isolate as fungal plant growth promoting agent. *Agronomy.* 2021;11:392. <https://doi.org/10.3390/agronomy11020392>.
- Ritpitakphong U, Falquet L, Vimolstut A, Berger A, Métraux J, L'Haridon F. The microbiome of the leaf surface of *Arabidopsis* protects against a fungal pathogen. *New Phytol.* 2016;210:1033–43. <https://doi.org/10.1111/nph.13808>.
- Satam H, Joshi K, Mangrolia U, Waghoos S, Zaidi G, Rawool S, Malonia SK. Next-generation sequencing technology: current trends and advancements. *Biology.* 2023;12:997. <https://doi.org/10.3390/biology12070997>.
- Segata N, Izard J, Waldron L, Gevers D, Miropolsky L, Garrett WS, Huttenhower C. Metagenomic biomarker discovery and explanation. *Genome Biol.* 2011;12:60. <https://doi.org/10.1186/gb-2011-12-6-r60>.
- Seybold H, Demetrowitsch TJ, Hassani MA, Szymczak S, Reim E, Hauelsen J, Lübbers L, Rühlemann M, Franke A, Schwarz K, Stukenbrock EH. A fungal pathogen induces systemic susceptibility and systemic shifts in wheat metabolome and microbiome composition. *Nat Commun.* 2020;11:1910. <https://doi.org/10.1038/s41467-020-15633-x>.
- Sohrabi R, Paasch BC, Liber JA, He SY. Phyllosphere Microbiome. *Annu Rev Plant Biol.* 2023;74:539–68. <https://doi.org/10.1146/annurev-arpla-nt-102820-032704>.
- Strobel G. The emergence of endophytic microbes and their biological promise. *J Fungi.* 2018;4:57. <https://doi.org/10.3390/jof4020057>.
- Swathy PS, Joshi MB, Mahato KK, Muthusamy A. He-Ne laser irradiation in brinjal leads to metabolic rewiring and accumulation of bioactive components in fruits. *Sci Hortic.* 2023;322:112400. <https://doi.org/10.1016/j.scienta.2023.112400>.
- Tao J, Cao P, Xiao Y, Wang Z, Huang Z, Jin J, Liu Y, Yin H, Liu T, Zhou Z. Distribution of the potential pathogenic *Alternaria* on plant leaves determines foliar fungal communities around the disease spot. *Environ Res.* 2021;200:111715. <https://doi.org/10.1016/j.envres.2021.111715>.
- Tedersoo L, Bahram M, Pöhlme S, Kõljalg U, Yorou NS, Wijesundera R, Abarenkov K. Global diversity and geography of soil fungi. *Science.* 2014;346:1256688. <https://doi.org/10.1126/science.1256688>.
- Trivedi P, Leach JE, Tringe SG, Sa T, Singh BK. Plant–microbiome interactions: from community assembly to plant health. *Nat Rev Microbiol.* 2020;18:607–21. <https://doi.org/10.1038/s41579-020-0412-1>.
- Vannier N, Agler M, Hacquard S. Microbiota-mediated disease resistance in plants. *Plos Pathog.* 2019;15:e1007740. <https://doi.org/10.1371/journal.ppat.1007740>.
- Venkatachalam S, Ranjan K, Prasanna R, Ramakrishnan B, Thapa S, Kanchan A. Diversity and functional traits of culturable microbiome members, including cyanobacteria in the rice phyllosphere. *Plant Biolo.* 2016;18:627–37. <https://doi.org/10.1111/plb.12441>.
- Větrovský T, Kohout P, Kopecký M, Machac A, Man M, Bahnmann BD, Brabcová V, Choi J, Meszárošová L, Human ZR, Lepinay C, Lladó S, López-Mondéjar R, Martinović T, Mašínová T, Morais D, Navrátilová D, Odriozola I, Štursová M, Švec K, Tláskal V, Urbanová M, Wan J, Žifčáková L, Baldrian P. A meta-analysis of global fungal distribution reveals climate-driven patterns. *Nat Commun.* 2019;10:5142. <https://doi.org/10.1038/s41467-019-13164-8>.
- Wang X, Radwan MM, Taráwneh AH, Gao J, Wedge DE, Rosa LH, Cutler SJ. Antifungal activity against plant pathogens of metabolites from the endophytic fungus *Cladosporium cladosporioides*. *J Agric food chem.* 2013;61:4551–5. <https://doi.org/10.1021/jf400212y>.
- Wang N, Stelinski LL, Pelz-Stelinski KS, Graham JH, Zhang Y. Tale of the Huanglongbing Disease pyramid in the context of the Citrus Microbiome. *Phyto Pathol.* 2017;107:380–7. <https://doi.org/10.1094/PHYTO-12-16-0426-RVW>.
- Wang S, Tan Y, Li S, Zhu T. Structural and dynamic analysis of leaf-associated fungal community of walnut leaves infected by leaf spot disease based Illumina high-throughput sequencing technology. *Pol J Microbiol.* 2022;71:429–41. <https://doi.org/10.33073/pjm-2022-038>.
- White TJ, Bruns T, Lee S, Taylor JW. Amplification and direct sequencing of fungal ribosomal RNA genes for phylogenetics. In: Innis MA, Gelfand DH, Sninsky JJ, White TJ, editors. *PCR protocols: a guide to methods and applications*. New York: Academic Press; 1990. p. 315–22.
- Xiong C, Zhu Y, Wang J, Singh B, Han L, Shen J, Li P, Wang G, Wu C, Ge A, Zhang L, He J. Host selection shapes crop microbiome assembly and network complexity. *New Phytol.* 2021;229:1091–104. <https://doi.org/10.1111/nph.16890>.
- Yan ZZ, Chen QL, Li CY, Thi Nguyen BA, He JZ, Hu HW. Contrasting ecological processes shape the *Eucalyptus* phyllosphere bacterial and fungal community assemblies. *J Sustain Agric Environ.* 2022;1:73–83. <https://doi.org/10.1002/sae2.12007>.
- Yang N, Zhang Y, Li J, Li X, Ruan H, Bhole P, Keiblinger K, Mao L, Liu D. Interaction among soil nutrients, plant diversity and hypogeal fungal trophic guild modifies root-associated fungal diversity in coniferous forests of Chinese Southern Himalayas. *Plant Soil.* 2022;481:395–408. <https://doi.org/10.1007/s11104-022-05646-4>.
- Zahn G, Amend AS. Foliar microbiome transplants confer disease resistance in a critically-endangered plant. *PeerJ.* 2017;5:e4020. <https://doi.org/10.7717/peerj.4020>.
- Zapka C, Leff J, Henley J, Tittl J, De Nardo E, Butler M, Edmonds-Wilson S. Comparison of standard culture-based method to culture-independent method for evaluation of hygiene effects on the hand microbiome. *M Bio.* 2017;8:10–1128. <https://doi.org/10.1128/mbio.00093-17>.
- Zhang Z, Luo L, Tan X, Kong X, Yang J, Wang D, Zhang D, Jin D, Liu Y. Pumpkin powdery mildew disease severity influences the fungal diversity of the phyllosphere. *Peer J.* 2018;6:e4559. <https://doi.org/10.7717/peerj.4559>.
- Zhang L, Zhang J, Wei Y, Hu W, Liu G, Zeng H, Shi H. Microbiome-wide association studies reveal correlations between the structure and metabolism of the rhizosphere microbiome and disease resistance in cassava. *Plant Biotechnol J.* 2021;19:689–701. <https://doi.org/10.1111/pbi.13495>.
- Zhou X, Wang JT, Wang WH, Tsui CK, Cai L. Changes in bacterial and fungal microbiomes associated with tomatoes of healthy and infected by *Fusarium oxysporum* f. sp. lycopersici. *Microb ecol.* 2021;81:1004–17. <https://doi.org/10.1007/s00248-020-01535-4>.
- Zhu Y, Xiong C, Wei Z, Chen Q, Ma B, Zhou S, Tan J, Zhang L, Cui H, Duan G. Impacts of global change on the phyllosphere microbiome. *New Phytol.* 2022;234:1977–86. <https://doi.org/10.1111/nph.17928>.